Theoretical Study of the Adsorption of Formaldehyde on Magnesium Oxide Nanosurfaces: Size Effects and the Role of Low-Coordinated and Defect Sites

ARTICLE *in* THE JOURNAL OF PHYSICAL CHEMISTRY B · NOVEMBER 2004

Impact Factor: 3.3 · DOI: 10.1021/jp0470546

3 AUTHORS:

Rita Kakkar
University of Delhi
110 PUBLICATIONS **583** CITATIONS
SEE PROFILE

Pramesh N Kapoor
University of Delhi
121 PUBLICATIONS **1,652** CITATIONS
SEE PROFILE

Kenneth Klabunde
Kansas State University
357 PUBLICATIONS **13,794** CITATIONS
SEE PROFILE

Theoretical Study of the Adsorption of Formaldehyde on Magnesium Oxide Nanosurfaces: Size Effects and the Role of Low-Coordinated and Defect Sites

Rita Kakkar* and Pramesh N. Kapoor

Department of Chemistry, University of Delhi, Delhi-110 007, India

Kenneth J. Klabunde

Department of Chemistry, Kansas State University, Manhattan, Kansas 66506

Received: July 5, 2004; In Final Form: September 14, 2004

The electronic and geometrical structures of nanoclusters of MgO have been investigated by density functional calculations. The dependence of the properties on size is studied. Defect formation energies are also calculated for various ionic and atomic vacancies. A study of the adsorption of formaldehyde at various sites has shown that the lower coordination sites are preferred so much that, in cases where the nanocluster can adapt itself to expose more of the lower coordination sites, it readily does so. A strong four-membered ring involving the carbonyl group and surface MgO units is formed. This results in a weakening of the carbonyl bond to almost a single bond. The adsorbed species is formate-like in structure, the second CO bond being formed with a surface oxide. The surface Mg−O bonds in the four-center complex are also considerably weakened. The adsorption process is highly exothermic. An investigation of adsorption of formaldehyde at defect sites has revealed that many interesting adsorption products are formed depending on the nature of the vacancy. Adsorption at these positions releases more energy than at perfect MgO surfaces.

1. Introduction

Metal oxide nanoparticles are highly active for a large number of reactions that are important in both pollution control and chemical synthesis.[1] The adsorption of formaldehyde on metal oxide surfaces has recently assumed importance after the observation that nanosized metal oxide particles have the capability to dissociatively adsorb toxic organic pollutants, including aldehydes and ketones.[2] In an effort to search for better materials to control environmental pollution and to control the quality of indoor air, we have here attempted to characterize the properties of the MgO surface and the mode of adsorption of formaldehyde on the MgO surface.

Magnesium oxide, an insulator, is considered a model system for solid state and surface studies because of its simple structure and ionic bonding. It also exhibits catalytic activity for a wide variety of reactions.[3−7] It has been established that the catalytic activity of magnesium oxide is due to a small number of defect sites (steps, kinks, corners, etc.) with surface ions, particularly oxygen, having low coordination numbers.[8−11] For example, the dissociative adsorption of hydrogen molecules on pairs of adjacent low-coordinated O^{2-} and Mg^{2+} ions takes place via a heterolytic cleavage of the H−H bond,[12−16] resulting in the formation of MgH^+ and OH^- surface groups. Theoretical and experimental studies have established a qualitative correlation between the chemical properties of the surface Mg−O pairs and their coordination numbers. The explanation for these correlations is that surface sites usually have low band gaps and ion charges, resulting in enhanced covalency of these low-coordinated sites, which facilitates electron transfer from the σ bonding orbital of H_2 to the surface, and from the surface to the σ^* antibonding orbital of hydrogen, cleaving the H−H bond and forming stronger O−H and Mg−H bonds.

Magnesium oxide is particularly interesting in nanoparticle form. It has been possible to prepare MgO in very high surface area (500 m^2/g) with average crystallite sizes of about 4 nm.[17] The high surface areas and the intrinsically high surface reactivity allows these materials to be especially effective as adsorbents;[8,9] in fact, they have been called "destructive adsorbents" because of their tendency to adsorb and simultaneously destroy, by bond-breaking processes, a series of toxic chemicals. For example, organophosphorus compounds (mimics of poisonous nerve agents) are destroyed at relatively low temperature and in high capacity. These nanoparticles are also effective for destruction of organochlorine compounds, and they adsorb large quantities of SO_2, CO_2, HCl, HBr, and other gases.[18−20]

Nanoscale MgO can be considered as a stoichiometric chemical reagent. Its high surface area implies that 30−40% of the MgO moieties are on the surface, thus allowing surface−gas reactions to occur approaching a stoichiometric range, and its electronic structure implies only s−p electrons. Magnesium oxide readily cleaves to expose the MgO(100) surface. It has thus been considered as an ideal system to study the catalytic properties of metal oxides.

In materials (metals, semiconductors, or insulators) where strong chemical bonding is present, delocalization can vary with size. This effect, coupled with structural changes with size variation, can lead to different chemical and physical properties, *depending on size.* Indeed, it has now been demonstrated that a host of properties depend on the size of such nanoscale particles, including magnetic and optical properties, melting points, specific heats, and surface reactivity.[21] Smaller and smaller particles may take on different crystalline forms or at least different morphologies and should possess more edge and corner sites (lower coordination sites), and this could affect their surface reactivities or adsorption properties.[22] Thus, the high activity of small particles may not be a simple surface area

* To whom correspondence should be addressed. E-mail: rita_kakkar@vsnl.com.

10.1021/jp0470546 CCC: $27.50
Published on Web 10/29/2004

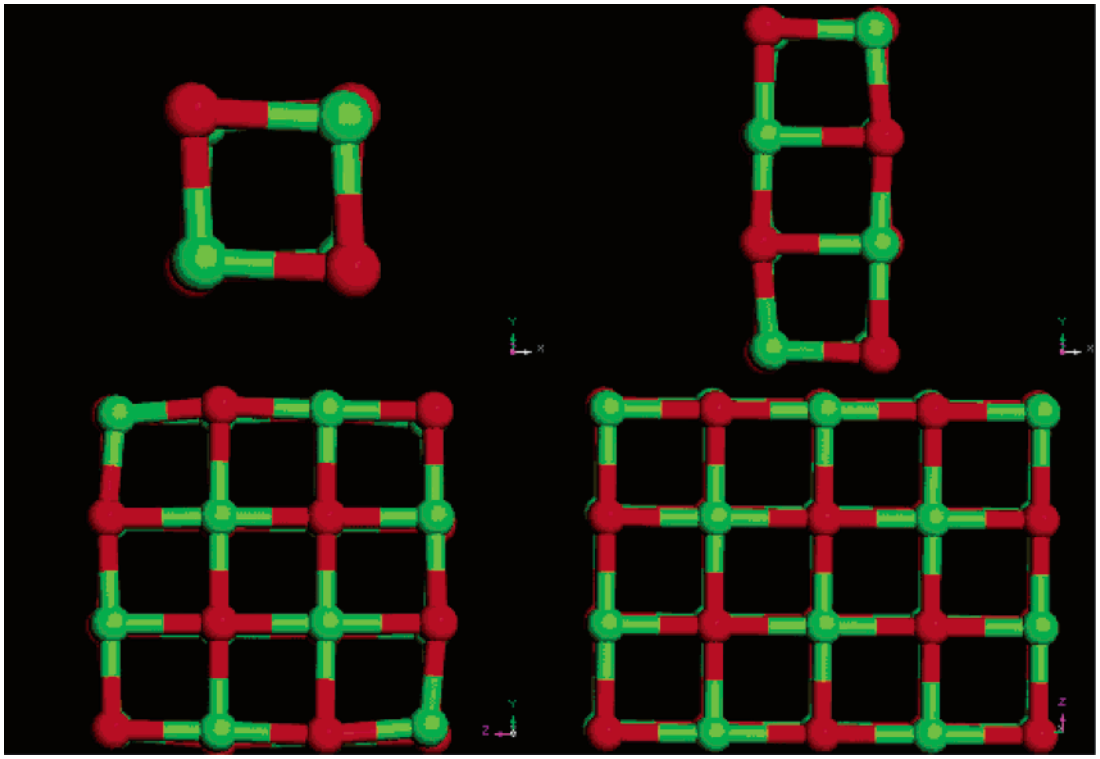

Figure 1. The $(MgO)_n$ clusters taken for the calculation. Here $n = 4$, 8, 16, and 20 clusters are shown. The 12-unit cluster is shown in subsequent figures. Color codes: Mg, green; O, red.

effect, but may also be due to the larger proportion of lower coordination sites as the crystallite size decreases. These lower coordination sites have higher-lying d-states, making them much more reactive, according to the d-band center model.[23]

Before a theoretical description of chemical reactions on the MgO surface can be undertaken, it is necessary to accurately represent the MgO bulk and surface properties, especially the energetics of removal of surface atoms and ions resulting in defects. Surfaces of cleaved, polished, powdered, and other types of MgO samples are very rough on the atomic scale and contain many steps and other low-coordinated sites, such as kinks and corners.[24,25] Several theoretical and experimental studies have been performed,[26−29] and in this work, we have compared our results of our accurate density functional calculations with these studies. We have organized the work as follows:

1. We have taken small clusters of increasing size to model the MgO nanoparticles and have compared the calculated surface relaxation and rumpling with previous theoretical and experimental values. The electronic properties of MgO have also been investigated with reference to the low-coordinated sites.

2. Surface defects arising from atom, ion, and MgO vacancies are then investigated.

3. Adsorption of a representative small molecule, formaldehyde, at various low-coordinated and defect sites is also investigated.

2. Computational Methods

First-principles density functional (DF) calculations were performed using the DMol^3 code[30] available from Accelrys Inc. in the Materials Studio 3.0 package. The exchange-correlation contribution to the total electronic energy was treated in a spin-polarized generalized-gradient corrected (GGA) form of the local density approximation (LDA),[31] with the Perdew−Burke−Ernzerhof (PBE) correlation.[32] Density functional calculations at the GGA level are expected to give good prediction for the bonding energies of carbonyl systems on the oxide surfaces.[31,33,34] Our calculations employed numerical basis sets of double-ζ quality plus polarization functions (DNP) to describe the valence orbitals of O, C, Mg, and H. The use of numerical basis sets minimizes the basis set superposition error (BSSE).[35]

To investigate possible size effects, the reaction enthalpies were computed on different sized stoichiometric crystals ranging from $(MgO)_4$ to $(MgO)_{20}$ (Figure 1), but subsequent adsorption studies were made on the $(MgO)_{12}$ cluster (Figures 2 and 3). A rectangular $(MgO)_{12}$ cluster has a size of about $0.6 \times 0.4 \times 0.2$ nm^3. This cluster exposes three-, four-, and five-fold sites. Previous calculations[36] have shown that this cluster size is adequate for these calculations.

Complete geometry optimizations for all structures, except where otherwise indicated, were carried out. Vibrational frequencies were calculated to confirm that the adsorption products are equilibrium structures on the potential energy surface. The charge distributions were estimated using the molecular electrostatic potential fitting approach.[37] Free valences and bond orders were calculated using Mayer's procedure,[38] since the Mulliken method has well-known shortcomings because of the uncertainty in uniquely defining a charge-partitioning scheme.[39]

3. Results

3.A. Surface Properties. *3.A.1. MgO(100) Relaxation and Rumpling.* It has been observed, both experimentally and theoretically,[40,41] that the (100) surfaces of many cubic ionic crystals, including the rock salt structures of alkali halides and MgO, experience a characteristic relaxation with respect to an ideal cleavage plane. Two features are common for this relaxation:

(i) the entire surface plane is displaced toward the bulk, decreasing the distance between the surface and the next layer, and

(ii) cations of the surface layer move toward the bulk more than anions, and this is known as rumpling.

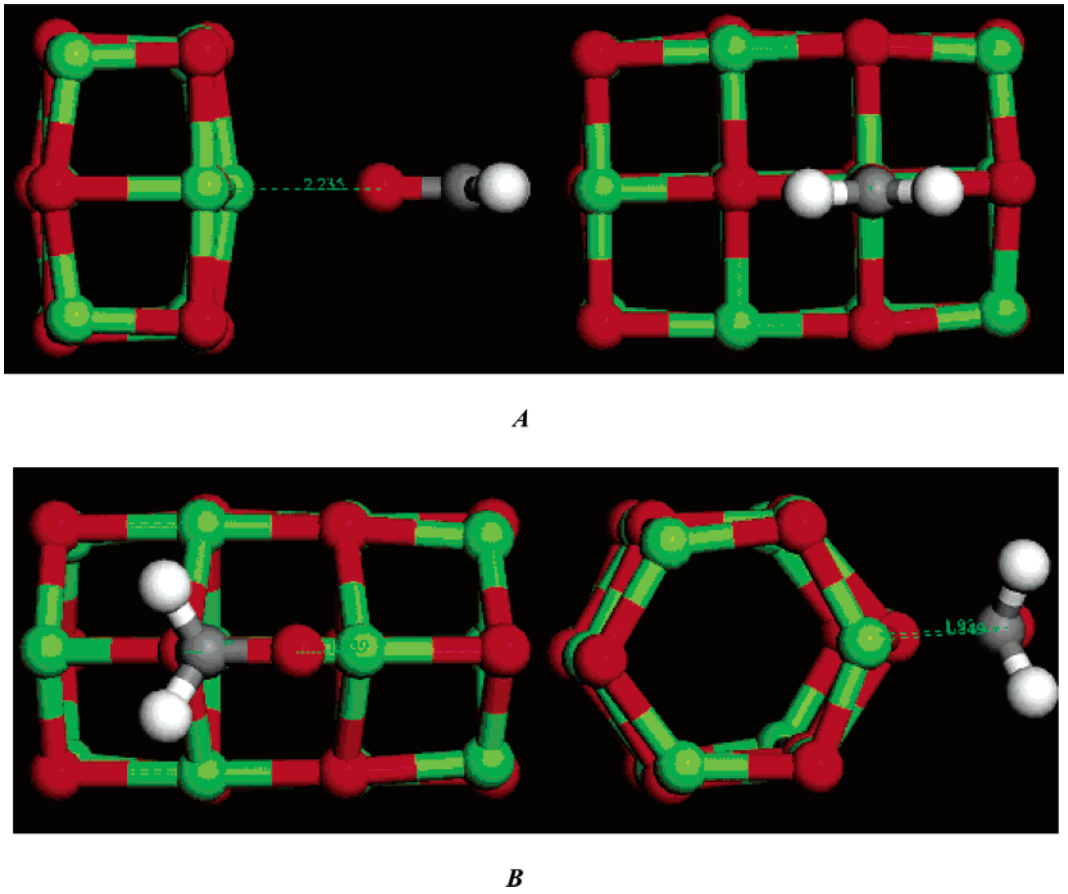

Figure 2. Two modes of adsorption of formaldehyde at the planar nanosurface. Two views: A, singly bonded to Mg; B, di-σ-bonded. Color codes: Mg, green; O, red; C, gray; H, white. As mentioned in the text, the 5c coordination site becomes 4c as a result of massive reconstruction of the surface in Mode B.

However, although there is considerable variation in the values of ionic displacements obtained in different studies, it is generally agreed that the relaxation and rumpling at the MgO(100) surface are small, the former being about −1%, while the latter is less than 4% of the lattice constant.

In this work, we have calculated the surface relaxation, rumpling, and relaxation energies for stoichiometric MgO clusters of various sizes (Table 1) and compared these with previous experimental and theoretical values. In our modeling of the MgO surface, we relaxed the whole system. Calculations were made for a series of clusters of increasing surface area and a thickness of two layers.

Surface relaxation (δd_{12}) is defined as the difference of the average vertical distance of the first-layer atoms to the second layer (d_{12}) from the bulk interlayer spacing, d (2.132 Å), and is given as a percentage of d. In this case, since both layers are surface layers, this quantity has been halved to calculate the displacement of each layer. The calculated surface relaxation depended on the size of the cluster. However, the values obtained for the larger clusters are in agreement with the most recent experimental measurements,[40,42] which gave values of ±1% for the surface relaxation. Theoretical studies[41,43−45] also predict a small surface relaxation, between +1% and −1%, in agreement with the range of experimental data for vacuum-cleaved surfaces.

Surface rumpling Δ_1 is defined as the difference of the mean vertical positions of oxygen and magnesium atoms in the first layer and is also given as a percentage of d. The calculated values for the surface rumpling (Table 1) are higher than the experimental values[40,42] of −0.5% to 1.6%. In all cases, the corner magnesium atoms moved inward by a greater amount, yielding rounded corners. The larger rumpling observed for smaller units is because of the larger proportion of corner sites. However, the calculated surface rumpling is in agreement with the most accurate theoretical values of +1% to +4%.[43−45] For the $(MgO)_{20}$ cluster, the average ionic displacements obtained from the ideal surface plane positions are 0.03 Å for anions and −0.05 Å for cations, that is, anions move up and cations down toward the bulk, in qualitative agreement with previous results. Notice that the cations move down by larger amounts than the anions move up, resulting in a net displacement toward the bulk.

The relaxation energy, E, has been defined as the difference in binding energy between the relaxed and nonrelaxed model and was normalized to the number of surface MgO units in the model. The surface relaxation energy per MgO unit decreases as the number of MgO units increases. Again, the decrease is on account of the smaller proportion of corner sites with increasing cluster size.

3.A.2. Electronic Properties of MgO(100). We also calculated the energies of the highest occupied molecular orbitals (HOMOs) and lowest unoccupied molecular orbitals (LUMOs) as a function of cluster size. As the number of surface MgO units is increased from 4 to 20, the energy of the HOMO changes only slightly (Table 2), but the LUMO energy increases considerably. Thus, the calculated HOMO−LUMO gaps increase from 2.41 eV for the 4 MgO unit cluster to 2.96 eV for the 20 unit cluster. The smaller band gaps for the smaller units therefore facilitate charge transfer to and from the adsorbent molecules. The magnitude of the Fermi energy per MgO unit

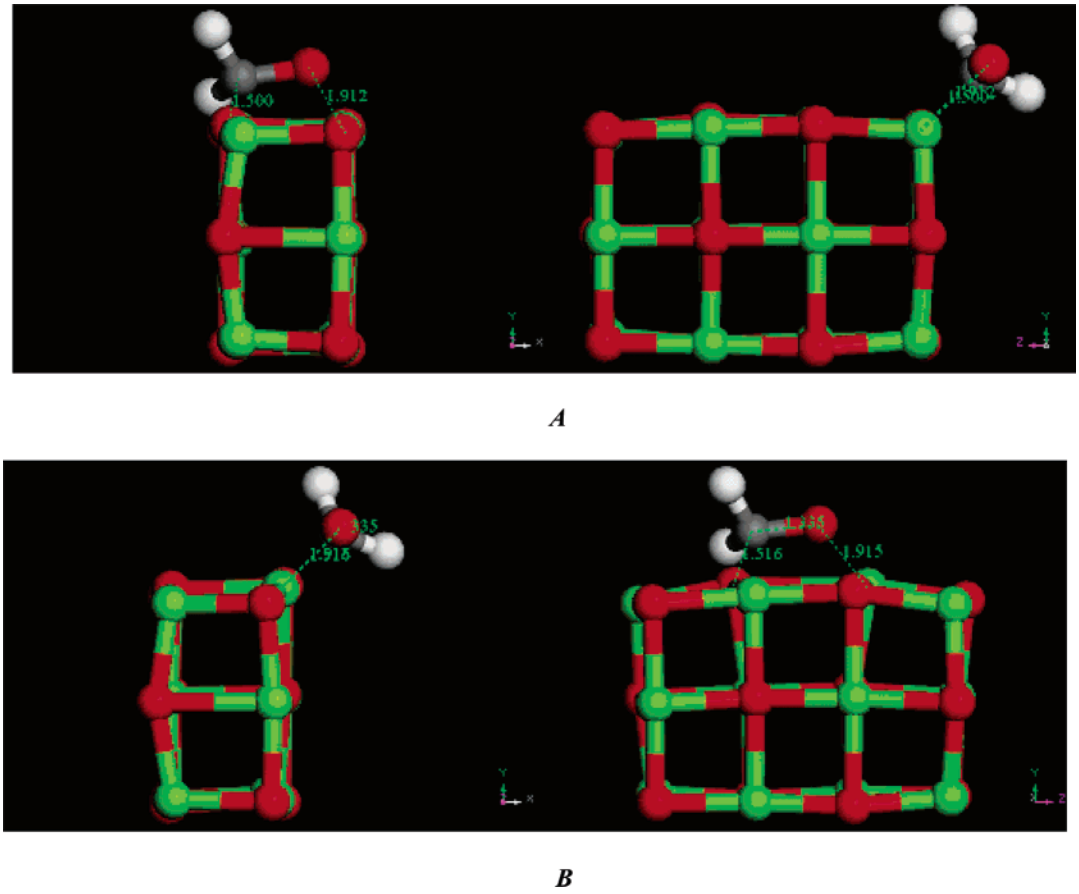

Figure 3. Two views of the low-coordinate magnesium oxide−formaldehyde adsorbed system. A: at 3c site; B: at 4c site. Adsorption at the 5c site is shown in Figure 2.

TABLE 1: Surface Relaxation δd_{12}, Rumpling Δ_1, and Relaxation Energy E for the MgO(100) Surface as a Function of the Number of MgO Units

no. of MgO units	δd_{12}	Δ_1	E
4	−3.8	5.0	50.2
8	−2.0	4.4	41.8
12	−0.9	4.1	33.6
16	−0.6	3.8	29.4
20	−0.3	3.6	27.1

TABLE 2: Calculated HOMO, LUMO, and Fermi Energies (eV) for the MgO(100) Surface as a Function of the Number of MgO Units

no. of MgO units	HOMO	LUMO	E_F
4	−4.73	−2.32	−3.45
8	−4.73	−2.06	−3.34
12	−4.77	−1.93	−3.29
16	−4.75	−1.87	−3.24
20	−4.78	−1.82	−3.22

decreases from −0.86 to −0.16 eV as the cluster size increases from 4 to 20 MgO units.

From Tables 1 and 2, it is clear that the $(MgO)_{12}$ unit cluster gives a fair representation of larger clusters and has exposed three-, four-, and five-coordinate sites. It was thus used for further calculations.

Bulk MgO is a highly ionic compound.[46,47] For the penta-coordinated Mg atoms in the surface, the calculated charge density (1.42) is smaller than that in hexacoordinated Mg atoms in the bulk (1.49). The calculated Mayer free valences (which are indices of reactivity) for the three-, four-, and five-coordinate magnesiums are, respectively, 1.83, 1.77, and 1.74. The higher covalency of the corner sites is thought to be responsible for the catalytic behavior of MgO.

3.A.3. Formation Energies of Oxygen Vacancies at Different Sites. As discussed above, smaller clusters exhibit unique behavior because of the larger proportion of lower coordinate sites, in particular, the three-coordinate corner sites. We now investigate anion vacancies at the MgO(100) surface and at the MgO corners. Although these certainly are very common surface defects that are claimed to be responsible for various physical and chemical surface processes,[48,49] their properties are not well established.

Three different oxygen positions have been considered, a corner site (O_{3c}), an edge site (O_{4c}), and the planar site (O_{5c}). The defect formation energy of a vacancy V_{Onc} is defined as

$$E_V(O_{nc}) = E(Mg_{12}O_{11}V_{Onc}) + E(O) - E(Mg_{12}O_{12})$$

Except the neutral oxygen atom (^3P), all electronic states in the above expression are singlet states (^1A). The literature results for E_V show large variations when different approaches are compared, for example, $E_V(O_{5c})$ varies from 756 to 1176 kJ/mol.[41,45,50−55] On the other hand, all three ab initio studies that compare the relative stability of different oxygen vacancy sites[51,52,55] agree that the energy $E_V(O_{5c})$ is highest, followed by $E_V(O_{4c})$ and $E_V(O_{3c})$. This trend is well reproduced in the present calculations, which predict defect formation energies of 767, 822, and 842 kJ/mol, respectively, for the three-, four-, and five-coordinated oxygen defects.

The interesting point is the considerable reduction in positive charges of the neighboring magnesium atoms from their initial values of 1.4. The three-coordinate and two-coordinate magnesium atoms, resulting from the oxygen vacancies, have charges of 0.49 and 0.39, respectively, resulting in higher covalency and reactivity.

TABLE 3: Calculated Vacancy Formation Energies E_V (kJ/mol) on the Planar MgO Nanosurface

	surface species				
defect	O_{5c}	O_{5c}^{2-}	Mg_{5c}	Mg_{5c}^{2+}	$(MgO)_{5c}$
nonrelaxed	861	3082	1030	2984	612
relaxed	842	2899	720	2675	341

TABLE 4: Comparison of Calculated Displacements (Å) of Nearest Magnesium and Oxygen Atoms after Formation of Oxygen Defects V_{O5c} for Different Methods[a]

	V_{O5c}		V_{O5c2-}	
atom	DFT	EMBED*	DFT	EMBED[b]
surface Mg	+0.15	+0.04	+0.43	+0.22
surface O	−0.05	0.0	−0.21	−0.13

[a] The defects are along the vector from the defect position in the atom. [b] From ref 54. Relaxation of the nearest neighbors

3.A.4. Formation of Charged and Neutral Vacancies on the Planar Surface. Vacancies of neutral and charged species, O_{5c}, O_{5c}^{2-}, Mg_{5c}, Mg_{5c}^{2+}, and $(MgO)_{5c}$, have been considered. The vacancy formation energies E_V are defined as follows:[54,56]

$$E_V(O_{5c}) = E(Mg_{12}O_{11}V_{O5c}) + E(O) - E(Mg_{12}O_{12})$$

$$E_V(O_{5c}^{2-}) = E(Mg_{12}O_{11}V_{O5c})^{2+} + E(O^{2-}) - E(Mg_{12}O_{12})$$

$$E_V(Mg_{5c}) = E(Mg_{11}O_{12}V_{Mg5c}) + E(Mg) - E(Mg_{12}O_{12})$$

$$E_V(Mg_{5c}^{2+}) = E(Mg_{11}O_{12}V_{Mg5c})^{2-} + E(Mg^{2+}) - E(Mg_{12}O_{12})$$

$$E_V(\{MgO\}_{5c}) = E(Mg_{11}O_{11}V_{O5c}V_{Mg5c}) + (1/12)\,E(Mg_{12}O_{12}) - E(Mg_{12}O_{12})$$

In the last expression, the average energy of one MgO unit has been taken as $^1/_{12}$ that of the 12-unit cluster.

The vacancy formation energies are very large (Table 3), particularly those for the charged species. Surface relaxation reduces the defect formation energies considerably, except for the neutral O_{5c} vacancy, which shows relatively small effect upon relaxation. In fact, even the charged O^{2-} vacancy shows little relaxation effects. Although our results are in qualitative agreement with the EMBED results,[54] the agreement is not so good for the O^{2-} vacancies, implying that there are larger effects of O^{2-} vacancies in nanosized particles.

The geometrical changes after formation of a neutral or charged oxygen vacancy are compared to those obtained with the EMBED method[54] in Table 4. The general trend that magnesium atoms move away from the defect position (indicated by positive displacements) while oxygen atoms move toward it are observed with both methods. The displacements are larger for V_{O5c2-} than for V_{O5c}, and our calculated values are larger than those obtained by Scorza et al.[54] since small particles are able to deform easily, leading to larger relaxations.

There are large changes in the electron distribution, too, particularly for neutral atom defects. For example, removal of a neutral oxygen, which had an electronic charge of −1.470 in the $(MgO)_{12}$ cluster, causes this charge to be distributed among the surrounding Mg atoms, which show a decrease in their positive charge from an average of 1.430 to an average of 0.711. In particular, the four-coordinate Mg atom has a positive charge of only 0.243. The average electronic charge on the nearest-neighbor oxygens also decreases from −1.437 to −1.079, implying that they too are responsible for the increase in the electron density on the magnesiums. Similarly, for the neutral Mg defect, the average charge density on the five oxygens to which it was originally bonded reduces to an average of −1.383 from an initial average of −1.463. The nearest-neighbor magnesium atoms gain electron density and their positive charge reduces to 0.938 from 1.456. In both cases, it is seen that the magnesiums suffer larger increases in electron density on vacancy formation.

The electron acceptor or donor properties of the nanosurface can be understood in terms of the changes in Fermi energies on vacancy formation. The Fermi energy of the perfect 12-unit MgO surface was calculated as −3.29 eV (Table 2). Upon removal of an O, Mg, and MgO, respectively, the Fermi energy changes to −2.62, −5.06, and −3.71 eV. It is easy to see that Mg defect sites will behave as electron acceptors, while O defect sites donate electron density to adsorbent molecules.

TABLE 5: Selected Geometric Parameters of Adsorbed and Isolated Formaldehyde

	Mode A	Mode B	formaldehyde
	bond lengths (Å)		
O−C	1.219	1.328	1.214
$C-H_1$	1.109	1.117	1.115
$C-H_2$	1.110	1.117	1.115
H_1--H_2	1.897	1.813	1.894
Mg--O	2.235	1.939	
O--C		1.549	
	bond angles (°)		
H_1-C-O	121.3	114.4	121.9
H_2-C-O	121.2	114.4	121.9
H_1-C-H_2	117.5	108.5	116.3
	dihedral angle (°)		
H_1-CO-H_2	180.0	126.0	180.0

3.B. Adsorption of Formaldehyde. Bonding of Formaldehyde to the Oxide Surface. *3.B.1. Orientation of Formaldehyde.* For studying the adsorption of formaldehyde on the metal oxide surface, we considered two bonding modes, Mode A, with the formaldehyde molecule singly bonded onto a magnesium atom (see Figure 2A), with the formation of a planar surface species, $Mg-O{=}CH_2$, and Mode B, in which the plane of the formaldehyde molecule is approximately parallel to the MgO-(100) surface, and the carbonyl group interacts with both the magnesium and oxygen atoms of MgO (see Figure 2B) through its oxygen and carbon, respectively.

For the five-coordinated sites, the adsorption energy (E_{ads}), calculated according to the expression

$$E_{ads} = E_{form} + E_{MgO} - E_{complex}$$

where E_{form} is the binding energy of isolated formaldehyde in its equilibrium configuration (−1646.2 kJ/mol), E_{MgO} is the total binding energy of the bare $(MgO)_{12}$ cluster (−10128.4 kJ/mol), and $E_{complex}$ is the total binding energy of the adsorbate/$(MgO)_{12}$ system, was 19.2 kJ/mol for Mode A of adsorption. In these calculations, complete geometry optimization was performed. The positive value for the adsorption energy implies that the adsorption process is exothermic. For Mode B, the adsorption energy was significantly higher, 124.8 kJ/ mol, indicating that this mode is definitely preferred. It is obvious from Figure 2B that considerable distortion of the cluster as well as the adsorbed molecule occurs in Mode B of interaction.

Table 5 contains the geometrical parameters of adsorbed and isolated formaldehyde. It can be seen that the adsorbed molecule undergoes distortion in Mode B of interaction but remains practically unchanged for Mode A, which can be considered as

TABLE 6: ESP Fitted Atomic Charges of Adsorbed and Isolated Formaldehyde

atom	Mode A	Mode B	V_{Osc}	V_{Mg5c}	V_{O2-5c}	V_{Mg2+5c}	V_{MgO5c}	free
O	−0.335	−0.923	−0.406	−0.441	−0.362	−0.882	−1.194	−0.359
C	0.220	1.132	−1.565	0.514	0.060	0.668	0.420	0.292
H_1	0.062	−0.157	0.392	0.019	0.020	−0.139	−0.035	0.033
H_2	0.065	−0.157	0.404	0.387	0.023	−0.134	0.157	0.033

TABLE 7: Adsorption Energies, E_{ads} (kJ/mol), and Distortion Energies, E_{dis} (kJ/mol), Obtained for the Adsorption of Formaldehyde at Various Sites (see Figures 2 and 3) on the MgO Surface

	$E_{ads}(1)^a$	$E_{ads}(2)^b$	E_{dis}(MgO)	E_{dis}(form)	E_{int}
$Mg_{5c}O_{5c}$	8	125	33	110	268
$Mg_{4c}O_{4c}$	30	91	113	119	323
$Mg_{3c}O_{3c}$	142	186	57	138	381

[a] Relaxation of formaldehyde only. [b] Complete geometry optimization.

TABLE 8: Optimized Surface Mg−O, Surface O−C, and Carbonyl CO Distances

	optimization 1[a]			optimization 2[b]		
	Mg−O	O−C	C−O	Mg−O	O−C	C−O
$Mg_{5c}O_{5c}$	2.735	2.895	1.218	1.939	1.549	1.328
$Mg_{4c}O_{4c}$	2.089	1.883	1.247	1.915	1.516	1.335
$Mg_{3c}O_{3c}$	1.956	1.572	1.335	1.909	1.502	1.363

[a] Relaxation of formaldehyde only. [b] Complete geometry optimization.

physisorption, since the adsorption energy is low and the Mg---O bond is long (the calculated Mg−O bond order is only 0.126). In Mode B, the C−O bond distance, in particular, increases by 0.11 Å, indicating a significant weakening of this bond on adsorption. In fact, the CO bond order decreases from 2.048 in isolated formaldehyde to 1.294 upon adsorption.

Further, it can be seen from Table 5 that, in Mode B, the HCH bond angle of adsorbed formaldehyde decreases by 8° with respect to free formaldehyde, and the two hydrogens of formaldehyde therefore get closer by 0.08 Å.

3.B.2. Charge Distribution. The calculated ESP fitted charges on the atoms of the formaldehyde moiety are given in Table 6. It can be again seen that there is a considerable polarization of charge in Mode B. The net charge on the formaldehyde moiety is 0.012 in Mode A, but it is −0.105 in Mode B. This suggests that, in Mode B of adsorption, there is a transfer of electron density from an oxide ion of the nanosurface to the π^* orbital of formaldehyde, weakening the carbonyl bond. The high negative charges on the carbonyl oxygen (−0.923) and on the bonded surface oxygen ion (−1.071) suggest that a carboxylate-like species is formed.

The atomic charges reported in Table 6 again reinforce our contention that Mode A of adsorption entails only molecular adsorption or physisorption, while Mode B involves chemisorption. Formaldehyde may initially interact via Mode A, but the binding energy is too small for the molecule to remain adsorbed in this mode for a long enough time for dissociation to take place. It may, therefore, immediately form a four-membered ring (Mode B) by the interaction of the positively charged carbonyl carbon with a negatively charged surface oxygen. The two possible modes have also been reported in the literature.[57] We have confined further studies to Mode B of adsorption, as this involves oxidation to carboxylate.

3.B.3. Effect of Coordination. We next considered the relative adsorption energies for various low-coordinated sites (Figure 3). Table 7 gives the calculated adsorption energies for formaldehyde at various sites on the MgO surface. The first column refers to the adsorption energy obtained for geometry optimization of only formaldehyde, keeping the MgO nanosurface fixed at the optimized value.

The results reported in the first column in Table 7 agree with the general trend that $E_{ads}(Mg_{3c}O_{3c}) > E_{ads}(Mg_{4c}O_{4c}) > E_{ads}(Mg_{5c}O_{5c})$, that is, lower coordination sites offer stronger adsorption. This is to be expected since, as we had observed, the mechanism of interaction involves the transfer of electron density from the nanosurface to the formaldehyde moiety, particularly the oxygen atom. As we have observed before (see section 3.A.2), the low-coordinated magnesium atoms have smaller positive charges, facilitating easy charge transfer to the oxygen of the carbonyl group.

Column 2 offers interesting results. As the $(MgO)_{12}$ cluster is allowed to relax, considerable increase in the adsorption energy takes place, particularly for the planar five-coordinate positions. To see the source of this increase, we separately calculated the distortion energies for the nanocluster and formaldehyde, calculated from the difference of single-point energies at the distorted geometry in the complex and the optimized energy of the molecules.

Thus,

$$E_{dis}(\text{MgO}) = E_{\text{MgO}}(\text{complex}) - E(\text{MgO})$$

$$E_{dis}(\text{form}) = E_{\text{form}}(\text{complex}) - E(\text{form})$$

$$E_{ads} = E_{int} - E_{dis}(\text{form}) - E_{dis}(\text{MgO})$$

where $E_{int} = E_{form}(complex) + E_{MgO}(complex) - E_{complex} = E_{ads} + E_{dis}(form) + E_{dis}(MgO)$.

For adsorption at the 5c site, the distortion energy of the MgO cluster is smaller than expected from the fact that it changes shape completely. Instead of a cuboid shape, it takes on a tubular shape (see Figure 2). Thus, the 5c site transforms itself to a 4c site. This is indicative of the huge preference for lower coordination sites. Smaller clusters are able to distort themselves in such a way as to decrease the coordination number of Mg and O at the adsorption site. The distortion energy is highest for adsorption at the 4c site. In all cases, the formaldehyde moiety undergoes considerable distortion, as the C═O bond polarizes to a C^+—O^- bond. The interaction energies increase considerably on going to lower coordination sites.

Table 8 gives the optimized Mg---O, O---C, and carbonyl CO distances for the two cases. The strongest adsorption is found at the corner three-coordinate sites. It is obvious that strong covalent bonds are formed between the surface Mg and O atoms and the carbonyl CO group, resulting in weakening of the latter. In fact, the calculated Mg--O (carbonyl), surface O—C, and CO (carbonyl) bond orders are 0.434, 0.717, and 1.176, respectively, signifying the considerable weakening of the carbonyl bond upon adsorption.

The decrease in the C═O bond order and formation of a new C−O bond is reflected in the calculated vibrational frequencies for adsorbed formaldehyde, which indicate carbon−oxygen bands at 1150 cm^{-1} (intensity = 164 km/mol) and 1490 cm^{-1} (intensity = 21 km/mol) replacing the calculated carbonyl band for free formaldehyde (1797 cm^{-1}, intensity = 107 km/mol).

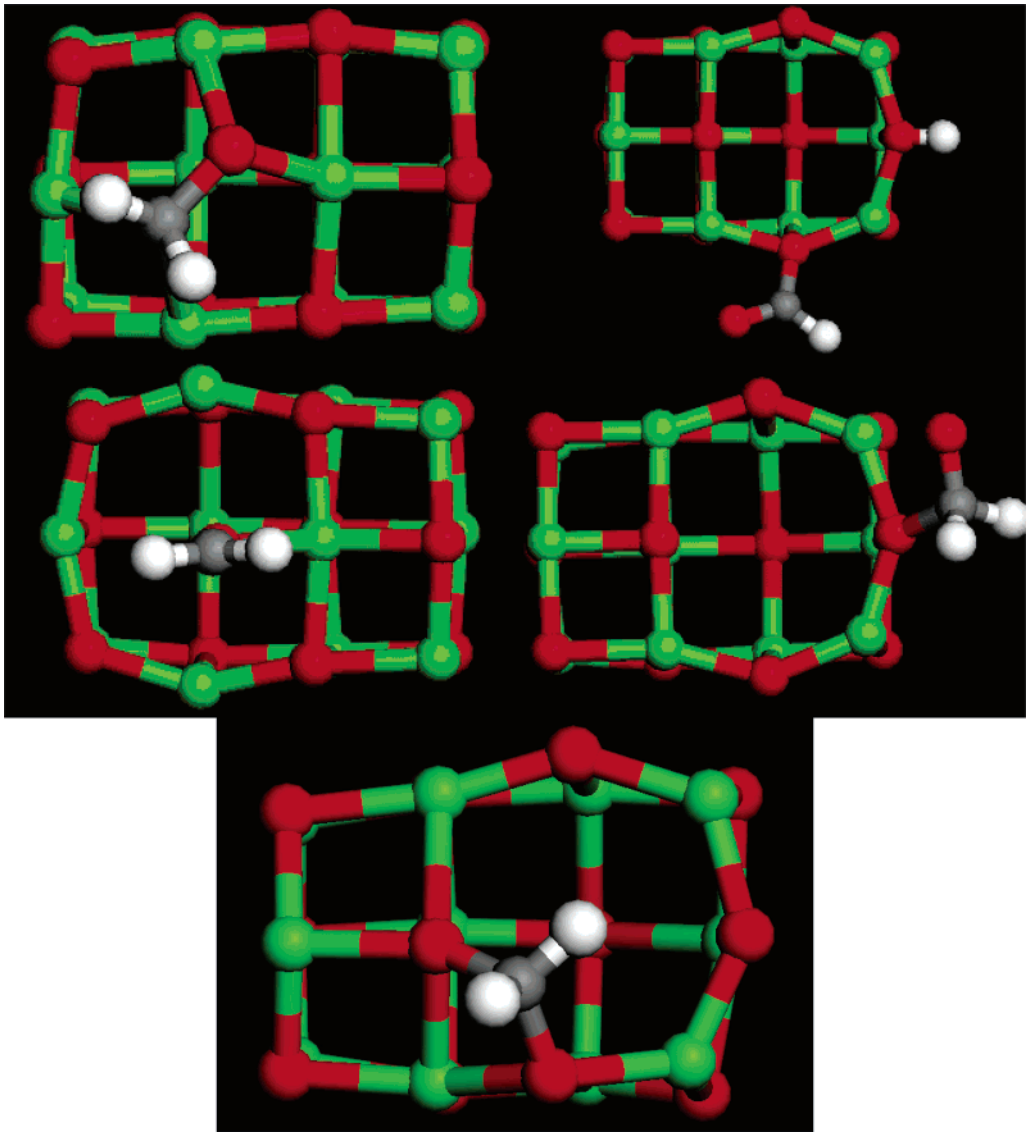

Figure 4. Geometries of the defect $(MgO)_{12}$ cluster−formaldehyde complexes. From left to right: Top row, O and Mg defects; Middle row, O^{2-} and Mg^{2+} defects; Bottom row, MgO defect.

The shift of the carbonyl band to lower frequency and the appearance of a new band at 1150 cm^{-1}, corresponding to a single C−O bond, is in perfect accord with our experimental observations from FTIR spectroscopy[2] for adsorption of acetaldehyde on MgO nanoparticles, which showed an increase in the ν_{CO} band at lower energy (1566 cm^{-1}), replacing the carbonyl band at 1761 cm^{-1} in free acetaldehyde, and the appearance of a new band at 1264 cm^{-1}, corresponding to the formation of C−O single bonds. On the basis of this evidence for acetaldehyde, some of us had suggested[2] the initial formation of a weak complex (Mode A), followed by the interaction of the positively charged carbonyl carbon with a basic oxygen ion surface site, resulting in the formation of a new C−O bond. This hypothesis is clearly validated by the present calculations. Moreover, the high exothermicity of the adsorption process and the multitude of products are reproduced in the present calculations. Ab initio calculations carried out previously[58] on the interaction of CO with MgO and CaO had also indicated a preference for four-membered ring systems over linear complexes in MgO.

3.B.4. Effect of Cluster Size. We next examined the effect of cluster size on the adsorption energies. Since the 3c site offered the strongest coordination, we determined the adsorption energies for adsorption of formaldehyde at this site for various sized clusters. The adsorption energies remain fairly constant with increase in cluster size, as the calculated adsorption energies are 190, 183, 186, 183, and 185 kJ/mol, respectively, for the 4-, 8-, 12-, 16-, and 20-MgO unit clusters, and there is no particular trend. The coordinating bond lengths also remain almost the same, the Mg--O bond length varying between 1.90 and 1.91 Å, and the O--C bond being between 1.49 and 1.50 Å. Hence, our calculations for the 12-unit cluster are representative of all cluster sizes.

3.B.5. Adsorption at Defect Sites. We also considered adsorption at various defect sites on the MgO surface, as it is well-known that these are responsible for the reactivity of MgO, since the perfect MgO surface is relatively inert. Again, O, O^{2-}, Mg, Mg^{2+}, and MgO vacancies arising from loss of these atoms/ions from the planar surface were considered as in section 3.A.4.

For the oxygen defect, the formaldehyde oxygen inserts itself into the vacant site, but slightly above the average plane of the other atoms (Figure 4). The high value of the adsorption energy (167 kJ/mol) shows that this is a highly exothermic process. The carbonyl bond weakens considerably and elongates by 0.3 Å to 1.453 Å, while the Mg---C and Mg---O bond lengths are 2.290 Å and 1.949 Å, respectively. The carbon is simultaneously

bonded to two Mg, two hydrogens, and the oxygen and has a high negative charge of −1.565. In section 3.A.4, we had mentioned that the Mg atoms move toward the defect sites on O removal, but, on insertion of the carbonyl oxygen, they move back to their original positions, and their mutual distance increases from 3.864 Å to 4.123 Å.

The product of formaldehyde adsorption at a Mg defect is even more interesting (see Figure 4). In this case, spontaneous dissociation takes place. There is a cleavage of a C−H bond. One of the low-coordination oxygens extracts a proton from formaldehyde. The relatively electron deficient carbon of the remaining HCO group is attracted to another three-coordinate oxide, forming a formate ($HCOO^-$) group with this oxide. The extra negative charge is absorbed by the nanosurface, which, as mentioned in section 3.A.4, is an electron acceptor. The adsorption energy is 208 kJ/mol.

Since both the neutral vacancies produce highly charged species, it is interesting to investigate charged ion defects. Accordingly, adsorption of formaldehyde on O^{2-} and Mg^{2+} vacancies was also considered. In the oxide defect (see Figure 4), the adsorption energy is rather low (87 kJ/mol), and the carbon does not become a part of the nanosurface. There is only a slight weakening of the carbonyl bond, which now has a length of 1.237 Å, and the net charge on the formaldehyde moiety is −0.259 (Table 6). For adsorption at a Mg^{2+} defect site, the adsorption energy is 137 kJ/mol. The electron deficient carbon of formaldehyde experiences an electrostatic attraction from a negatively charged surface oxygen (see Figure 4) to form a complex, in which the formaldehyde moiety has a net charge of 0.487 (see Table 6), indicating a charge transfer from formaldehyde to the nanosurface, in agreement with our earlier observations (see section 3.A.4).

Finally, adsorption of formaldehyde on a neutral MgO defect was investigated. The product here is somewhat similar to that for the neutral O defect, and the oxygen inserts itself into the O vacancy, remaining bonded to carbon, which acquires a tetrahedral structure, being bonded to two oxygens and two hydrogens (see Figure 4). The nanosurface acquires a hexagonal shape (as for the planar surface of perfect MgO), the oxygens dissociating themselves from the magnesiums and reducing their coordination number. This reaction is the most exothermic, as the heat of reaction is −301 kJ/mol.

Thus, we have several different products depending on the type of vacancy. The only case where a surface oxide extracts a hydrogen atom in the form of a proton from formaldehyde is in a neutral Mg defect.

These results can be interpreted in terms of the electron acceptor or donor nature of the defect surface (see section 3.A.4). In the oxygen defect, the nanosurface donates 1.173 *e* to formaldehyde, resulting in the carbon becoming electron-rich. The negative charge on the formaldehyde oxygen and high positive charges on the carbon and protons makes this a very polar structure (see Table 6). On the other hand, in the Mg defect, the formaldehyde moiety transfers 0.479 *e* to the nanosurface, and the resulting proton combines with a surface oxide to form a hydroxyl group, while the remaining HCO combines with another surface oxide to form a formate ($HCOO^-$) group.

4. Discussion

We have found several modes of adsorption for formaldehyde on the MgO nanosurface. Depending upon the coordination and the kind of defect site, different adsorption products are formed and all the reactions are highly exothermic. The low-coordination sites (particularly the corner 3c sites) are highly reactive and adsorb the formaldehyde molecule, which is di-σ-bonded, the oxygen of the carbonyl coordinating with an acidic Mg surface site, and the carbonyl carbon coordinating to the basic oxygen, leading to a four-coordinate complex in which the carbonyl bond is considerably weakened. A net transfer of electron density to formaldehyde takes place during the adsorption.

However, the reactions at defect sites yield even more thermodynamically stable products, particularly for neutral atom vacancies. The most exothermic are the reactions at a MgO defect site (301 kJ/mol) and Mg defect (208 kJ/mol). In both cases, electron density is withdrawn by the nanosurface from formaldehyde. In the latter, the withdrawal of electron density is enough to cause the activation of a C−H bond, leading to protonation of a basic oxide surface site.

Charged ion defect sites are relatively less reactive. This is explained as follows: If the average charge densities on oxide and magnesium atoms on the perfect surface are −1.4 and +1.4, respectively, an oxygen defect, for example, leads to 1.4 *e* of charge originally on that atom to be redistributed among the neighboring magnesium atoms, which become less positively charged and hence more covalently reactive. However, if an oxide ion is removed, there is only +0.6 of charge to be adjusted in the cavity. For the perfect surface and the oxygen defect, there is a net transfer of electron density to formaldehyde, while for Mg and MgO defects, it is the reverse, leading to different products.

In a very recent paper,[59] it has been suggested that there is spontaneous dissociation at the 3c coordinate site, leading to a heterolytic cleavage of a C−H bond, forming a proton bonded to a surface oxide and COH^- bonded to Mg. However, except at the Mg defect, protonation of a surface oxide is never found to occur. Moreover, experimental data[2] also do not support this product. In light of the paper, we performed several geometry optimizations with different starting geometries, but they always converged to the structures reported here. Even when the starting geometry had a hydrogen separated from a surface oxygen by 1.0 Å, the hydrogen moved away from the surface and the geometry converged to the structure reported here after several optimization steps. In the calculations reported in the paper,[59] extremely small cluster sizes (4, 6, and 8 units) were taken for the study, and the clusters were also not subjected to geometry optimization. Our calculations have indicated that relaxation of the geometry plays a substantial role in the adsorption process, and, unless it is allowed to relax, no adjustment for optimum interactions can occur. Further, the GGA functional, coupled with numerical basis sets, is expected to give a better description of the interactions than the hybrid functional used in that study.

The different products obtained illustrate the fascinating world of nanochemistry and explain the high reactivity of nanoparticles, as well as the capability of accurate density functional calculations to reproduce their behavior.

5. Conclusions

In conclusion, we may state that

- Formaldehyde chemisorbs onto the MgO surface, producing zwitterionic four-membered rings, in which the carbonyl CO bond is considerably weakened.
- Lower coordination sites are definitely preferred over the planar five-coordinate sites and form stronger bonds with the carbonyl moiety, resulting in the weakening of surface Mg−O bonds.
- In the adsorption at five-coordinate sites, unless severe reconstruction of the surface occurs, no chemisorption takes

place. The reconstruction makes the surface take on a cylindrical shape, reducing the coordination number of the surface Mg and O atoms.

• A myriad of different adsorption products is formed at different neutral atom defect sites, as the nanosurface may act as an electron donor or acceptor, depending on the type of vacancy.

The results obtained in this work provide a significant advance to our knowledge of chemistry at nanosurfaces. They provide a rationale for the high activity of these surfaces, since they have a larger proportion of the active low-coordination sites than regular metal oxides. The role of defect sites in the adsorption and dissociation process is also clearly indicated.

References and Notes

(1) Kapoor, P. N.; Bhagi, A. K., Mulukutla, R. S.; Klabunde, K. J. *Dekker Encyclopedia of Nanoscience & Technology;* Marcel Dekker: New York, 2004.
(2) Khaleel, A.; Kapoor, P. N.; Klabunde, K. J. *Nanostruct. Mater.* **1999**, *11*, 459.
(3) Shido, T.; Asakura, K.; Iwasawa, Y. *J. Catal.* **1990**, *122*, 55.
(4) Knözinger, E.; Jacob, K.-H.; Hofmann, P. *J. Chem. Soc., Faraday Trans.* **1993**, *89*, 1101.
(5) Ito, T.; Lunsford, J. H. *Nature* **1985**, *314*, 721.
(6) Driscoll, D. J.; Martir, W.; Wang, J. X.; Lunsford, J. H. *J. Am. Chem. Soc.* **1985**, *107*, 58.
(7) Ito, T.; Wang, J.; Lin, C. H.; Lunsford, J. H. *J. Am. Chem. Soc.* **1985**, *107*, 5062.
(8) Klabunde, K. J.; Stark, J.; Koper, O.; Mohs, C.; Park, D. G.; Decker, S.; Jiang, Y.; Lagadic, I.; Zhang, D. *J. Phys. Chem.* **1996**, *100*, 12142.
(9) Stark, J. V.; Park, D. G.; Lagadic, I.; Klabunde, K. J. *Chem. Mater.* **1996**, *8*, 1904.
(10) Boudart, M.; Delbouille, A.; Derouane, E. G.; Indovina, V.; Walters, A. B. *J. Am. Chem. Soc.* **1972**, *94*, 6622.
(11) Kunz, A. B.; Guse, M. P. *Chem. Phys. Lett.* **1977**, *45*, 18.
(12) Hattori, H.; Tanaka, Y.; Tanabe, K. *J. Am. Chem. Soc.* **1976**, *98*, 4652.
(13) Coluccia, S.; Boccuzzi, F.; Ghiotti, G.; Morterra, C. *J. Chem. Soc., Faraday Trans. 1* **1982**, *78*, 2111.
(14) Ito, T.; Sekino, T.; Moriai, N.; Tokuda, T. *J. Chem. Soc., Faraday Trans. 1* **1981**, *77*, 2181.
(15) Ito, T.; Kuramoto, M.; Yoshioka, M.; Tokuda, T. *J. Phys. Chem.* **1983**, *87*, 4411.
(16) Ito, T.; Murakami, T.; Tokuda, T. *J. Chem. Soc., Faraday Trans. 1* **1983**, *79*, 913.
(17) Utamapanya, S.; Klabunde, K. J.; Schlup, J. R. *Chem. Mater.* **1991**, *3*, 175.
(18) Li, Y. X.; Klabunde, K. J. *Langmuir* **1991**, *7*, 1388.
(19) Koper, O.; Li, Y. X.; Klabunde, K. J. *Chem. Mater.* **1993**, *5*, 500.
(20) Li, Y. X.; Schlup, J. R.; Klabunde, K. J. *Langmuir* **1991**, *7*, 1394.
(21) Klabunde, K. J.; Mohs, C. In *Chemistry of Advanced Materials: An Overview*; Interrante, L. V., Hampden-Smith, M. J., Eds.; Wiley-VCH: New York, 1998.
(22) Itoh, H.; Utamapanya, S.; Stark, J. V.; Klabunde, K. J.; Schlup, J. R. *Chem. Mater.* **1993**, *5*, 71.
(23) Ruban, A.; Hammer, B.; Stloltze, P.; Skriver, H. L.; Nørskov, J. K. *J. Mol. Catal. A: Chem.* **1997**, *115*, 421.
(24) Gallagher, M. C.; Fyfield, M. S.; Cowin, J. P.; Joyce, S. A. *Surf. Sci.* **1995**, *339*, L909.
(25) Abriou, D.; Creuzet, F.; Jupille, J. *Surf. Sci.* **1996**, *352*−*354*, 499.
(26) Sauer, J.; Ugliengo, P.; Garrone, E.; Saunders: V. R. *Chem. Rev.* **1994**, *94*, 2095.
(27) Pacchioni, G. *Surf. Rev. Lett.* **2000**, *7*, 277; *Solid State Sci.* **2000**, *2*, 161.
(28) Ménétrey, M.; Markovits, A.; Minot, C.; Pacchioni, G. *J. Phys. Chem. B* **2004**, *108*, 12858.
(29) Sushko, P. V.; Shluger, A. L.; Catlow, C. R. A. *Surf. Sci.* **2000**, *450*, 153.
(30) Delley, B. *J. Chem. Phys.* **1990**, *92*, 508; **2000**, *113*, 7756.
(31) White, J. A.; Bird, D. M. *Phys. Rev. B* **1994**, *50*, 4954.
(32) Perdew, J. P.; Burke, K.; Ernzerhof, M. *Phys. Rev. Lett.* **1996**, *77*, 3865.
(33) Ziegler, T. *Chem. Rev.* **1991**, *91*, 651.
(34) van Santen, R. A.; Neurock, M. *Catal. Rev.—Sci. Eng.* **1995**, *37*, 557.
(35) Matsuzawa, N.; Seto, J.; Dixon, D. A. *J. Phys. Chem. A* **1997**, *101*, 9391.
(36) Branda, M. M.; Belelli, P. G.; Ferullo, R. M.; Castellani, N. J. *Catal. Today* **2003**, *85*, 153.
(37) Singh, C. U.; Kollman, P. A. *J. Comput. Chem.* **1984**, *5*, 129.
(38) Mayer, I. *Int. J. Quantum Chem.* **1986**, *29*, 477.
(39) Wiberg, K. B.; Rablen, P. R. *J. Comput. Chem.* **1993**, *14*, 1504.
(40) Robach, O.; Renaud, G.; Barbier, A. *Surf. Sci.* **1998**, *401*, 227.
(41) Gerson, A. R.; Bredow, T. *Phys. Chem. Chem. Phys.* **1999**, *1*, 4889.
(42) Zhou, J. B.; Lu, H. C.; Gustafsson, T.; Häberle, P. *Surf. Sci.* **1994**, *302*, 350.
(43) Towler, M. D.; Harrison, N. M.; McCarthy, M. I. *Phys. Rev. B* **1995**, *52*, 5375.
(44) Li, Y.; Langreth, D. C.; Pederson, M. R. *Phys. Rev. B* **1997**, *55*, 16456.
(45) Finocchi, F.; Goniakowski, J.; Noguera, C. *Phys. Rev. B* **1999**, *59*, 5178.
(46) Sousa, C.; Illas, F.; Bo, C.; Poblet, J. M. *Chem. Phys. Lett.* **1993**, *215*, 97.
(47) Mejías, J. A.; Márquez, A. M.; Fernándes Sanz, J.; Fernándes-García, M.; Ricart, J. M.; Sousa, C.; Illas, F. *Surf. Sci.* **1995**, *327*, 59.
(48) Ferrari, A. M.; Pacchioni, G. *J. Chem. Phys.* **1997**, *107*, 2066.
(49) Paganini, M. C.; Chiesa, M.; Giamello, E.; Coluccia, S.; Martra, G.; Murphy, D. M.; Pacchioni, G. *Surf. Sci.* **1999**, *421*, 246.
(50) Gibson, A.; Haydock, R.; LaFemina, J. P. *Appl. Surf. Sci.* **1993**, *72*, 285.
(51) Kantorovich, L. N.; Holender, J. M.; Gillan, M. J. *Surf. Sci.* **1995**, *343*, 221.
(52) Castanier, E.; Noguerra, C. *Surf. Sci.* **1996**, *364*, 1.
(53) Orlando, R.; Millini, R.; Perego, G.; Dovesi, R. *J. Mol. Catal. A* **1997**, *119*, 253.
(54) Scorza, E.; Birkenheuer, U.; Pisani, C. *J. Chem. Phys.* **1997**, *107*, 9645.
(55) Pacchioni, G.; Pescarmona, P. *Surf. Sci.* **1998** *412/413*, 657.
(56) Ojamäe, L.; Pisani, C. *J. Chem. Phys.* **1998**, *109*, 10984.
(57) Henrich, V. E.; Cox, P. A. *The Surface Science of Metal Oxides;* Cambridge University Press: New York, 1994.
(58) Utamapanya, S.; Ortiz, J. V.; Klabunde, K. J. *J. Am. Chem. Soc.* **1989**, *111*, 799.
(59) Xu, Y.-J.; Zhang, Y.-F.-; Lu, N.-X.; Li, J.-Q. *Physica B* **2004**, *348*, 190.